PAPER

Investigating the kinetics of the formation of a C Cottrell atmosphere around a screw dislocation in bcc iron: a mixed-lattice atomistic kinetic Monte-Carlo analysis

View the article online for updates and enhancements.

Investigating the kinetics of the formation of a C Cottrell atmosphere around a screw dislocation in bcc iron: a mixed-lattice atomistic kinetic Monte-Carlo analysis

R Candela[1,2,*] , **S Gelin**[3], **N Mousseau**[4], **R G A Veiga**[5], **C Domain**[6,2],
M Perez[7] **and C S Becquart**[1,2,*]

[1] Univ. Lille, CNRS, INRAE, Centrale Lille, UMR 8207-UMET-Unité Matériaux et Transformations, F-59000 Lille, France
[2] Laboratoire commun EDF-CNRS Etude et Modélisation des Microstructures pour le Vieillissement des, Matériaux (EM2VM), France
[3] Département de Mathématiques et de Génie Industriel and Regroupement Québécois sur les Matériaux de Pointe, Polytechnique Montréal, Case Postale 6079, Succursale Centre-Ville, Montreal (QC) H3C 3A7, Canada
[4] Département de Physique and Regroupement Québécois sur les Matériaux de Pointe, Université de Montréal, Case Postale 6128, Succursale Centre-Ville, Montreal (QC) H3C 3J7, Canada
[5] Universidade Federal do ABC, Center for Engineering, Modeling, and Social Applied Sciences (CECS), Av dos Estados, 5001, Santa Terezinha, CEP 09210-580, Santo André/SP, Brazil
[6] EDF-R & D, Département Matériaux et Mécanique des Composants (MMC), Les Renardières, F-77818, Moret sur Loing Cedex, France
[7] Université de Lyon, INSA-Lyon, MATEIS, UMR CNRS 5510, 25 Avenue Jean Capelle, F-69621, Villeurbanne, France

E-mail: romain.candela@hotmail.fr and charlotte.becquart@univ-lille.fr

CrossMark

Abstract
We present a mixed-lattice atomistic kinetic Monte-Carlo algorithm (MLKMC) that integrates a rigid-lattice AKMC approach with the kinetic activation-relaxation technique (k-ART), an off-lattice/self-learning AKMC. This approach opens the door to study large and complex systems adapting the cost of identification and evaluation of transition states to the local environment. To demonstrate its capacity, MLKMC is applied to the problem of the formation of a C Cottrell atmosphere decorating a screw dislocation in α-Fe. For this system, transitions that occur near the dislocation core are searched by k-ART, while transitions occurring far from the dislocation are computed before the simulation starts using the rigid-lattice AKMC. This combination of the precision of k-ART and the speed of the rigid-lattice makes it possible to follow the onset of the C Cottrell atmosphere and to identify interesting mechanisms associated with its formation.

S Supplementary material for this article is available online

(Some figures may appear in colour only in the online journal)

---

* Authors to whom any correspondence should be addressed.

1. Introduction

Understanding the mechanisms that control defect and impurity diffusion in metals is crucial to characterize and predict the evolution of their mechanical properties. Yet, these processes occur on multiple length and time scales, from the angström to the metre, from the nanosecond to the year, raising significant challenges for both experimentalists and modellers. Consider, for example, the ageing process in steels, a major technological issue. The main mechanism at the origin of static strain ageing is the formation of Cottrell atmospheres (Cottrell and Bilby 1949): over time, carbon atoms, initially forming a solid solution in steels, segregate towards dislocations that act as sinks for solutes to form Cottrell atmospheres. This higher concentration of C hinders the motion of dislocations, which leads to the experimentally-observed hardening of the material (De *et al* 2000).

With the help of recently developed experimental and numerical tools, the study of Cottrell atmospheres was rekindled in the last two decades. Experimentally, it is now possible to observe directly an atmosphere with the atom probe field ion microscopy technique (Blavette 1999), (Smith *et al* 2013), (Wilde *et al* 2000), (Miller 2006). Cottrell atmospheres can also be modelled at the atomic scale with a metropolis Monte-Carlo approach (Veiga *et al* 2015), (Waseda *et al* 2017). However, observing the kinetics of the formation of a Cottrell atmosphere remains a challenge both experimentally and numerically, as saturation of the dislocation may take many months (Massardier *et al* 2004).

Computationally, the standard method for studying atomistic kinetics is molecular dynamics (MD). However, with a 1 to 5 fs timestep, MD is generally restricted to simulation times of the order of the μs at most. To circumvent that limitation, modelers have turned to kinetic Monte-Carlo (KMC) methods, based on an algorithm that focuses on activated mechanisms and can reach times up to seconds and even months depending on the selected system. Standard KMC methods are built on diffusion event catalogues that must be constructed ahead of the simulation, with atoms moving on rigid crystalline lattices. This approximation fails for distorted systems, such as in the vicinity of a dislocation, with high concentrations of defects and disordered regions.

The kinetic activation-relaxation technique (k-ART), an off-lattice KMC algorithm with on-the-fly catalogue building capabilities (El-Mellouhi *et al* 2008), (Béland *et al* 2011), lifts these limitations. K-ART is based on the open-ended event searching method ART nouveau, a very efficient method for exploring the local energy landscape (Mousseau and Barkema 1998), (Barkema and Mousseau 1996), (Malek and Mousseau 2000) and NAUTY (McKay 1981), a topological-analysis library for event classification. K-ART can correctly predict the kinetics of distorted systems such as C diffusion close to dislocation loops (Candela *et al* 2018), vacancy and C interaction in bulk Fe (Restrepo *et al* 2016) and long-time relaxation after ion-bombardment (Béland *et al* 2013). Treatment of distorted or disordered environment is costly, however, every step requires thousands of force evaluations, reducing k-

ART's efficiency for systems with a large number of mobile defects.

Since standard KMC is unable to correctly represent the formation of Cottrell atmospheres near a dislocation core and k-ART cannot deal with large number of mobile defects, we propose here to combine these two approaches, building on their respective strengths. As we demonstrate below, coupling the standard rigid-lattice approximation KMC with k-ART in a mixed-lattice KMC (MLKMC) opens the door to study complex systems with both precision and efficiency.

This is accomplished by spatially dividing the system in two zones, a rigid-lattice and an off-lattice zones, each with its own kinetics. Near the dislocation where the energy landscape is unknown, k-ART is used to search the possible transitions and compute the C migration energy barriers (k-ART zone). Far from the dislocation core, where C diffusion is well understood and can be described accurately using the rigid-lattice approximation, transitions are drawn from a standard KMC catalogue and migration energies are estimated with a model that accounts for carbon–carbon interactions and anisotropic elastic deformations of the lattice. After a detailed description of this non-trivial coupling, which deals mostly with the interface between these two regions, we show how MLKMC can provide unique insights into the fundamental steps in the formation of Cottrell atmospheres.

2. The mixed-lattice kinetic Monte-Carlo (MLKMC)

Figure 1 illustrates how MLKMC combines the speed of rigid-lattice KMC with the precision of k-ART to describe the kinetics of atoms in inhomogeneous systems: in regions where the rigid-lattice approximation no longer holds, such as near a dislocation core, k-ART is used to identify the possible transitions and relax them according to local deformations; on the other hand, where the rigid-lattice and k-ART predict the same results, such as in low-defect concentration crystalline regions, away from the dislocation, the rigid-lattice KMC approximation is used for its speed as, depending on the system, rigid-lattice KMC can be 10^5 to 10^9 faster than k-ART.

We discuss the technical aspects of the MLKMC in this section. Firstly, we describe the rigid-lattice KMC and k-ART in some details and in the context of C diffusion in Fe; for a detailed k-ART description, see for instance (El-Mellouhi *et al* 2008), (Béland *et al* 2011). We then present the MLKMC, with a focus on how best to determine the k-ART zone size and conclude the algorithmic presentation by describing the implementation of the interface between the different lattices. An example of an MLKMC step and the validation of the method is provided in the supplementary material (https://stacks.iop.org/JPCM/33/065704/mmedia) for a better understanding.

2.1. Search for transitions and computation of C migration energies

2.1.1. Transitions in the rigid-lattice zone. The rigid-lattice approximation is the standard approach for atomistic KMC
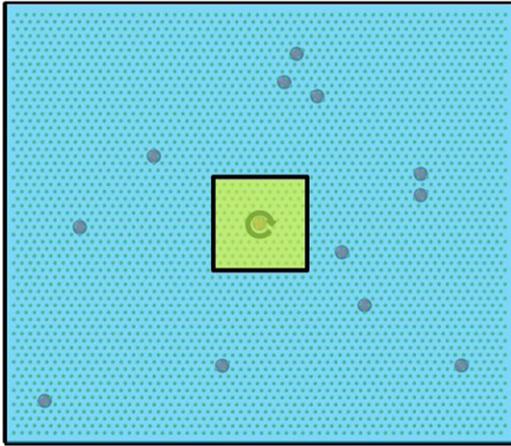
Figure 1. Representation of the k-ART zone (yellow) and the rigid-lattice zone (blue) composing a simulation box. The system consists of C atoms (large circles) immersed in a bulk bcc Fe crystal (small circles) containing a screw dislocation (circular arrow in the middle of the simulation box). Transitions are searched with k-ART for the C atoms in the k-ART zone, and with the rigid-lattice approximation for the C atoms in the rigid-lattice zone.

Figure 2. Energy of a C–C pair (E_{C-C}) versus the distance between the C atoms. At the distance $d = a_0 = 2.855\,32$ Å, the energy of the configuration equals 0.9 eV when a Fe atom is found between the C atoms, and 0.1 eV otherwise. Note that C atoms at a distance of 2.85 Å have two possible energies, depending on whether a Fe atom is present or not between the two C atoms.

(AKMC) simulations. By placing atoms on a grid and restraining the possible jumps to the nodes of this grid, the transitions can be computed before the simulation starts and catalogued as a function of the occupation. The migration energies for these transitions are estimated here using a simple model which guarantees the speed of the method while taking into account carbon–carbon interactions and deformations of the lattice induced by the dislocation.

In the model developed for the rigid-lattice zone, only moves associated with the migration of C atoms are included in the catalogue: C jumps from an octahedral site (O site) to an adjacent O site through a tetrahedral site (T site), which corresponds to the saddle point. The migration energy for this transition is computed according to:

$$E_{migC} = E^0_{migC} + \frac{\Delta E_{C-C}}{2} + \Delta E_{distortion}, \qquad (1)$$

where E^0_{migC} represents the C migration energy for a C atom in a perfect bcc lattice, $\frac{\Delta E_{C-C}}{2}$ the C–C interactions and $\Delta E_{distortion}$, the impact of the distortion of the system on the C migration energies.

Going more into details, E^0_{migC} is predicted to be 0.814 eV with the potential used here. This potential, which uses the embedded atom method (EAM), was developed by Becquart *et al* (Becquart *et al* 2007) and later slightly modified by Veiga and colleagues (Veiga *et al* 2014).

$\frac{\Delta E_{C-C}}{2}$, the corrective term associated to the C–C repulsion, is computed using a final-initial state energy model (Vincent *et al* 2008) also called a kinetically resolved activation (Van der Ven *et al* 2001) model. This model, based on the Kang and Weinberg decomposition of the migration energy (Kang and Weinberg 1989), is especially suitable to study the migration of point defects. As such, the corrective term can be written:
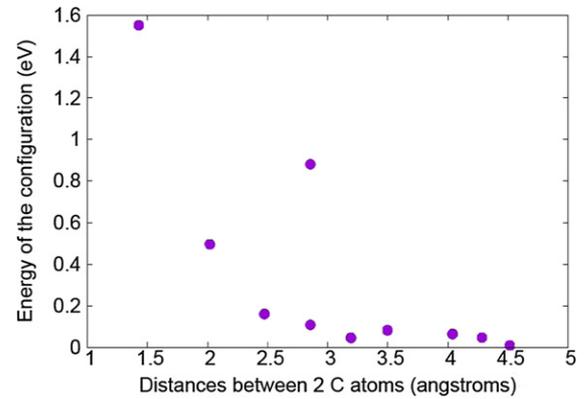
$$\Delta E_{C-C} = E_{final} - E_{initial} \qquad (2)$$

where E_{final} is the energy of the configuration after the C jump and $E_{initial}$ is the energy of the initial state. These energies are computed for several C–C distances according to equation (3):

$$E_{C-C} = E_{supercell\ with\ 2C\ interacting}$$
$$- E_{supercell\ with\ 2C\ not\ interacting} \qquad (3)$$

where E_{C-C} can represent either E_{final} or $E_{initial}$ of equation (2). With this definition, a positive value indicates a repulsive configuration. The results are presented in figure 2.

It is important to observe on figure 2 that E_{C-C} has two possible values for a C–C distance of $a_0 = 2.855\,32$ Å depending on whether the two C atoms share a Fe atom first nearest neighbour or not. A C atom in an O site distorts the Fe matrix mostly in one direction given by the C atom and its two nearest Fe neighbours. Having a configuration where 2 C atoms are separated by 2.85 Å with a Fe first nearest neighbour in-between results in the distortion induced by the two C atoms concentrated in one line (the $\|\overrightarrow{Fe_1C}\|$ line in figure S1. From the supplementary materials); when the two C atoms do not share a Fe first nearest neighbour, the distortion is more spread. For a better visualization of this issue, see for instance (Domain *et al* 2004—section 4 1 (figure 5)).

$\Delta E_{distortion}$ is introduced to account for the elastic deformation of the system (caused for example by dislocations) on the C migration energies; it is well known that the distortion of the system has a large influence on the migration energies of moving species (Veiga *et al* 2010), (Tchitchekova *et al* 2014), (Liu *et al* 2011), (Li *et al* 2011). The impact of a dislocation on C migration energies is computed with the method proposed by Veiga *et al* (Veiga *et al* 2011):

$$\Delta E_{distortion} = E^{binding}_{C_O-dislocation} - E^{binding}_{C_T-dislocation}, \qquad (4)$$

where $E^{binding}_{C_O-dislocation}$ represents the binding energy between the dislocation and a C atom in an O site and $E^{binding}_{C_T-dislocation}$, the binding energy between the dislocation and a C atom in a
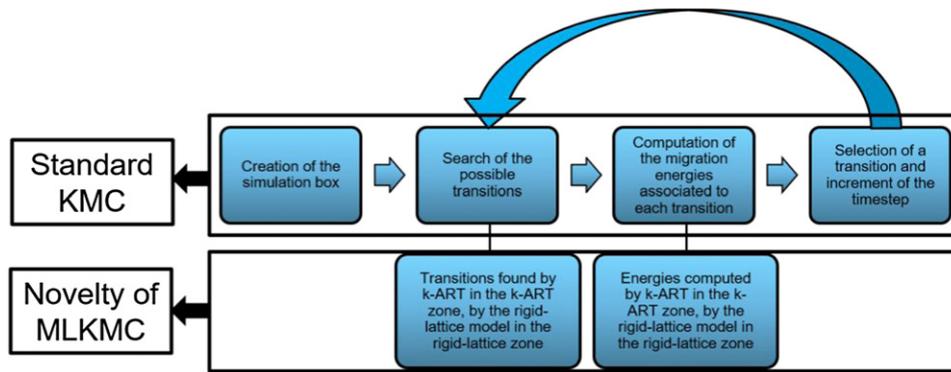
Figure 3. Overview of the MLKMC algorithm showing the different calls of k-ART and the rigid-lattice algorithm.
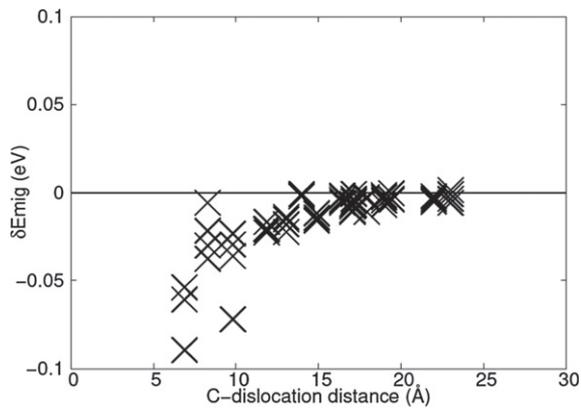

Figure 4. Difference in the C migration energies predicted by k-ART and by the rigid-lattice model (noted δE_{mig}) for different configurations containing 1 C atom and a screw dislocation. The migration energies are presented for different C-dislocation distances. The minimal C-dislocation distance is shown at 6 Å because for shorter C-dislocation distances, jumps of C atoms do not simply reduce to the usual 4 jumps, which imposes to use k-ART.
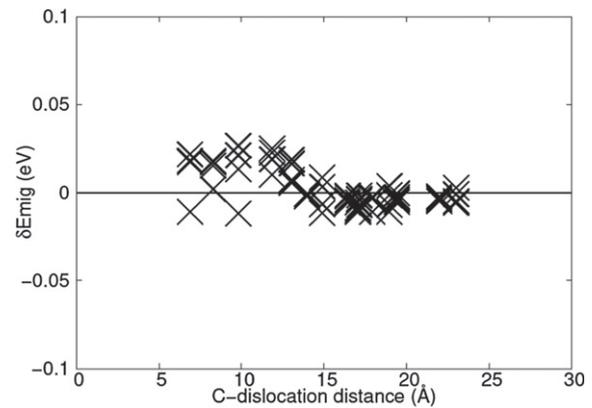

Figure 5. Difference in the C migration energies predicted by k-ART and by the rigid-lattice model (noted δE_{mig}) for different configurations containing 1 C atom and a screw dislocation, with $E^{binding}_{C_T-dislocation}$ computed with an atomistic model. The migration energies are presented for different C-dislocation distances.

T site. These energies are computed within the anisotropic elasticity theory using the Babel code (Clouet 2007).

2.1.2. Off-lattice transitions. The k-ART is an off-lattice/self-learning AKMC developed by one of us and collaborators (El-Mellouhi *et al* 2008), (Béland *et al* 2011). K-ART is based on the open-ended transition searching method activation relaxation technique nouveau (ART nouveau) (Barkema and Mousseau 1996), (Malek and Mousseau 2000), coupled with a topological classification for catalogue building (McKay 1981) and the standard KMC algorithm for bringing the time forward.

Contrary to string methods such as the NEB, ART nouveau requires the knowledge of only one local energy minimum and can identify the minimum energy paths connecting a configuration to its adjacent minima. ART proceeds in three steps to find a transition state. Firstly, ART applies a localised deformation on a local energy minimum to bring the system outside of the harmonic basin surrounding this minimum; then the system is moved along the eigendirection corresponding to the negative eigenvalue of the Hessian matrix until it converges onto an adjacent energy saddle point (activation step). Finally,

the system is relaxed into another energy minimum (relaxation step).

Using NAUTY, a topological analysis package (McKay 1981), k-ART classifies the local environment around each atom by assigning a key describing the local graph formed by links drawn between nearby atoms, typically at the first-neighbour distance. All atoms with the same topology are supposed to have the same event list this can be verified and corrected when it is not the case, as explained in (Béland *et al* 2011). For each topology, k-ART launches a larger number of ART nouveau searches (typically between 30 and 60) and generated events are stored in the catalogue. At each step, k-ART updates the list of active topologies, launching event searches, if needed, to complete the catalogue. A first tree of generic events is drawn, with an activation rate computed for each event using its activation energy and a constant prefactor; all events that have a KMC probability of 0.0001 or more to be selected are fully reconstructed and the saddle point is reconverged to ensure that the exact energy barrier is obtained (forming the specific events). Total rate for this final set of events (specific plus unrelaxed generic) is computed and the clock is incremented using an exponential distribution, with an event selected at random with a probability determined by its activation rate. As described elsewhere, k-ART includes a
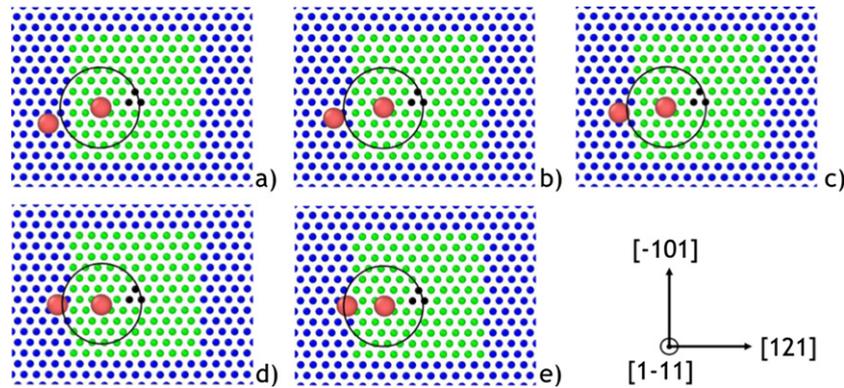
Figure 6. 5 steps (a–e) of an MLKMC simulation. On this simulation, the blue (green) circles represent Fe atoms in the rigid-lattice (k-ART) zone, the dark circles represent the screw dislocation (in the centre of the k-ART zone), and large red circles, C atoms. The circle around the C atom situated in the k-ART zone represents the topology cut-off of the C atom, larger than the cut-off of the potential (usually around 6 Å). The C atom in the bulk does 4 successive steps until it arrives within the topology cut-off of the C atom of the k-ART zone.

number of features to handle flickers, alloys, etc and it has been applied to a wide range of complex materials from self-defects in semiconductors and metals to impurities, grain boundaries and disordered and amorphous materials (Mousseau *et al* 2015), (Brommer *et al* 2014), (Restrepo *et al* 2018).

2.2. Overview of the MLKMC

The MLKMC algorithm integrates the two different KMC approximations described above in the same KMC event tree. An overview of the algorithm is presented in figure 3. We start by presenting how the simulation is setup and then discuss the details of the coupling between the rigid-lattice and the off-lattice region, the central contribution of MLKMC.

2.2.1. Determine the size of the k-ART zone. Determining the size of the off-lattice zone is a crucial point for an MLKMC simulation. Finding transitions and computing their migration energies in the k-ART zone is at least 10^5 times slower than doing it in the rigid-lattice zone, so the off-lattice region should be as limited as possible. The definition of the off-lattice region is largely controlled by the quality of the rigid-lattice approximation.

To determine the size of the off-lattice zone, we perform a preliminary characterization focussing on the diffusion mechanisms of interest. Here, for example, we evaluate the C diffusion barrier for several sites as a function of distance to the screw dislocation. The differences between the barriers predicted by k-ART and by the rigid-lattice model (noted δE_{mig}) for these configurations are presented in figure 4. In a perfect bcc Fe matrix, a C atom can perform 4 different jumps from its O site to neighbouring O sites with the T site being the saddle point. In figure 4, the smallest C-dislocation distance shown is at 6 Å because smaller distances lead to more complex C diffusion mechanisms than the four usual O–T–O jumps, thus requiring the use of k-ART.

As seen in figure 4, for C-dislocation distances lower than 12 Å, the migration energies predicted by k-ART can differ from the ones predicted by our rigid-lattice model by at least 50 meV, as previously shown by Veiga and colleagues (Veiga *et al* 2011). With this level of precision, the k-ART zone

should be, at the minimum, a rectangular parallelepiped with a square base centred on the dislocation and a 12 Å × 2 = 24 Å length. The k-ART zone is not chosen to be a circle or a hexagon for a better control of the interface, and especially to avoid interface issues such as an atom virtually in the k-ART zone and the rigid-lattice zone simultaneously.

It is possible to further reduce the off-lattice region by including continuous elasticity corrections to the rigid-lattice approximation. Veiga *et al* showed that the anisotropic elasticity fails to match atomistic results for the prediction of C migration energies for C-screw dislocation distances lower than 12 Å due to the anisotropic elasticity inability to predict accurate C-dislocation binding energies for a C atom at the saddle point between two O sites (Veiga *et al* 2011). To extend the validity of the rigid-lattice, these binding energies $E_{\mathrm{C_T-dislocation}}^{\mathrm{binding}}$ (equation (4)) are computed with the EAM potential used here instead of the anisotropic elasticity for C-dislocation distances comprised between 6 and 12 Å. This correction reduces the discrepancies in the C migration energies predicted by k-ART and by the rigid-lattice model observed in figure 4, leading to the match of k-ART and rigid-lattice model predictions observed in figure 5.

With improved barrier predictions for the rigid-lattice model, a rectangular parallelepiped with a square base centred on the dislocation whose length is 6 Å × 2 = 12 Å is now sufficient to enclose the k-ART region.

2.2.2. Interface between the rigid-lattice and the off-lattice zones. The kinetics internal to both the rigid-lattice and the off-lattice regions is correctly handled by the algorithms described above. The continuity between the k-ART and the lattice-based KMC parts must still be addressed, however. Continuity requires: (1) that detailed balance is respected as atoms move from one zone the other and (2) that the presence of atoms on one side of the interface correctly affects the kinetics on the other side.

Detailed balance

Detailed balance, also called microscopic reversibility, is a condition often imposed on studied systems to ensure their
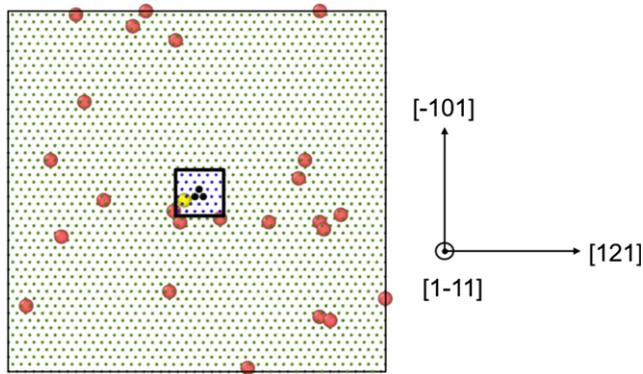
Figure 7. Example of a configuration studied by MLKMC containing 25 C atoms and a screw dislocation in the centre of the box. The large red (yellow) circles identify C atoms in the rigid-lattice (k-ART) zone, small green (blue) circles, Fe atoms in the rigid-lattice (k-ART) zone. The screw dislocation is represented by the three circles in black at the centre of the box. The small black square at the centre of the box represents the limits of the k-ART zone.

Figure 8. Representation of the three zones for the characterization of the Cottrell atmosphere formation: k-ART zone (red square), second ring (blue circle) and the third ring (green, rest of the box).

dynamical evolution reaches a steady-state equilibrium distribution. In practice, it means that the KMC algorithm must satisfy equation (5):

$$\pi_i Tr_{ij} = \pi_j Tr_{ji} \tag{5}$$

where π_i is the equilibrium probability distribution of state i and Tr_{ij} the transition rate from state i to state j.

For the MLKMC to respect this condition, detailed balance must be respected in the off-lattice zone, the rigid-lattice zone and at the interface between the two. In k-ART, detailed balance is guaranteed by ensuring that the initial-saddle-final configuration triplet forming the events are fully connected and by placing both forward and reverse events in the catalogue. In lattice-based KMC, detailed balance is also imposed by construction: as events are described as C jumps from an O site to an adjacent O site, when a possible event is found, its inverse event is also found at the same time and added in the list of possible events; the elastic corrections presented in the previous subsection do preserve the detailed balance.

To ensure detailed balance between the zones, atoms on one side of the interface correctly influence those on the other side of the interface. Formally, this is can be achieved by updating the positions of C atoms after each jump. However, for MLKMC, taking into account in k-ART the position of C atoms far from the dislocation after each move in the lattice-based region would require in a global energy minimization at each step, thus losing the advantage of the lattice-based KMC. As we have shown above, however, C movements in the bulk, far from the dislocation, have negligible impact on the migration energies of C atoms in the k-ART zone. Therefore, the position of C atoms in bulk region are provided to k-ART only after a k-ART jump or when a C atom moves near enough to the k-ART zone to modify the topological graph defined the local environment of C atoms in the on-lattice region. While this distance is system-depended, here it means that a full system relaxation is performed after every k-ART move or whenever a C atom moves in the rigid-lattice zone within 6 Å of
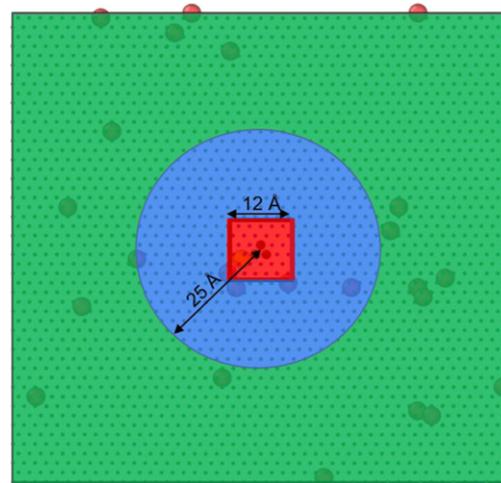
a C atom in the k-ART zone, as illustrated in figure 6. Note that like in figure 6, the figures presenting configurations are 2-dimensional cuts of a 3-dimensional configuration with the dislocation line perpendicular to the figure.

3. Results: MLKMC study of the 25 C-screw dislocation system

Ten simulations containing each 25 C atoms randomly placed (except one placed in the k-ART zone close to the dislocation) in a 36 000 α-Fe matrix (150 ppm in C) with a screw dislocation ($\vec{b} = \frac{a_0}{2}<111>$, with $\vec{b}$ the Burgers vector representing the deformation induced by the dislocation) are launched using the MLKMC at 300 K. Periodic boundary conditions are applied only in the dislocation line direction, free surfaces are applied on the other directions (C atoms are forbid to cross the free surfaces as events in the rigid-lattice catalogue are found between close O sites only). The basin mean rate method (Béland *et al* 2011), a method to treat small neighbouring barriers as a small basin getting rid of flickers, is activated with an energy barrier of 0.4 eV for an event to be considered within a basin. 60 event searches per topology are performed in the k-ART zone. All events centred on Fe atoms are rejected. The orientation of the system is ([121][−101][1−11]). The simulation box size is set to (104.9 × 100.9 × 39.6) Å^3, and the k-ART zone size, to (12.5 × 12.5 × 39.6) Å^3. An example of a configuration is shown in figure 7.

To characterize the formation of a Cottrell atmosphere, the simulation box is divided in three fictious parts: the k-ART zone, the second ring (a cylinder centred on the dislocation with a radius of 25 Å, minus the k-ART zone), and the third ring (corresponding to the rest of the box). These zones are represented in figure 8. The average evolution in time of the number of C atoms in these different zones is plotted to observe the influence of the screw dislocation on the C distribution in figure 9.
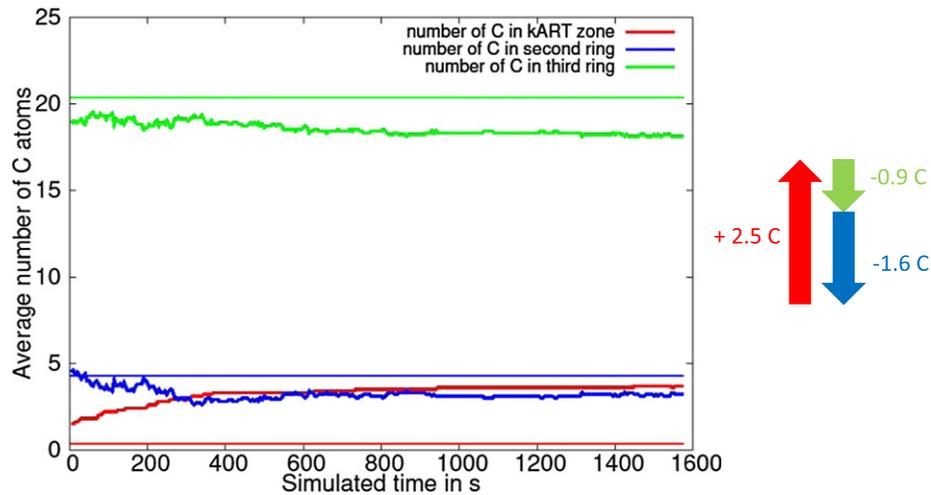
Figure 9. Average number of C atom per zone versus time for the MLKMC simulations containing 25 C atoms at 300 K with a screw dislocation in a 36 000 Fe matrix. The three zones defined are: the k-ART zone (red), the second ring (blue) and the third ring (green). The straight lines represent the concentration of C atoms per zone if the C atoms were in solid solution. The arrows represent the average C displacement between the beginning and the end of the simulations: the k-ART zone has been enriched with 2.5 C atoms on average, while the 2nd and 3rd rings have been depleted of respectively 1.6 and 0.9 C atoms on average.
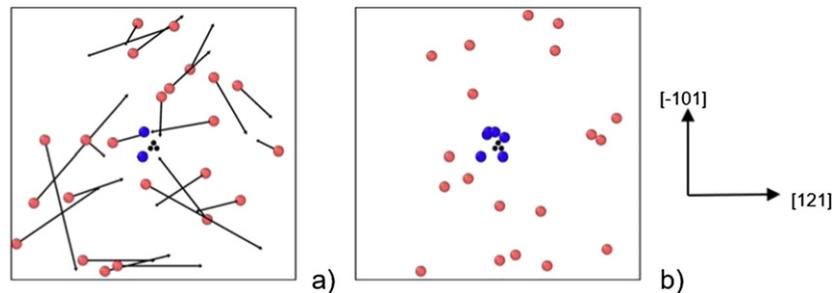

Figure 10. Initial (a) and final (b) configurations of an MLKMC simulation containing a screw dislocation and 25 C atoms at 300 K. The blue circles represent the C atoms in the k-ART zone, the red circles are the C in the rigid-lattice zone and the dark circles represent the screw dislocation. Arrows in (a) indicate the C displacement between the initial and the final configurations. Computational details: each simulation requires a CPU time of 13 days per core (16 cores) for a simulated time of 0.43 h and 22 000 steps (not counting the steps operated though the flicker-handling algorithm).
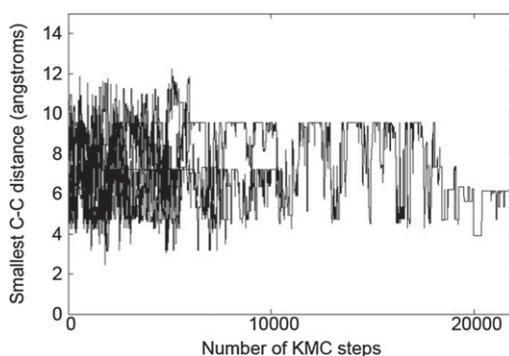

Figure 11. Smallest C–C distance observed for MLKMC simulations at 300 K containing a screw dislocation and 25 C atoms versus the number of steps of the simulation. A step corresponds approximatively to 70 ms, for a total simulated time is 1550 s.

Figure 9 shows that C atoms in the second ring tend to arrive relatively quickly to the dislocation line: in less than 1600 s, 2.5 C atoms on average arrived from the second ring to the dislocation line, while the second and the third ring have been

depleted of respectively 1.6 and 0.9 C atoms on average. This diffusion raises the C concentration in the k-ART zone surrounding the dislocation to a higher value than the average solid solution concentration (150 ppm) as the other zones are depleted in C atoms.

This concentration continues to increase with time, as shown by the ever-increasing red line, demonstrating the onset of a Cottrell atmosphere surrounding the dislocation. This is clearly seen when comparing initial and final configurations of the simulation (figure 10): in less than 1600 s (simulated time) at 300 K, several C atoms arrived from the bulk to the vicinity of the dislocation. While it can take up to a few months for a Cottrell atmosphere to be saturated at 300 K (Massardier *et al* 2004), MLKMC simulations predict that the first steps in the formation of a Cottrell atmosphere can be observed in less than an hour. This fast aggregation of C atoms close to the dislocation could lead to an increase in the Peierls stress occurring at the early stages of the formation of the Cottrell atmosphere.
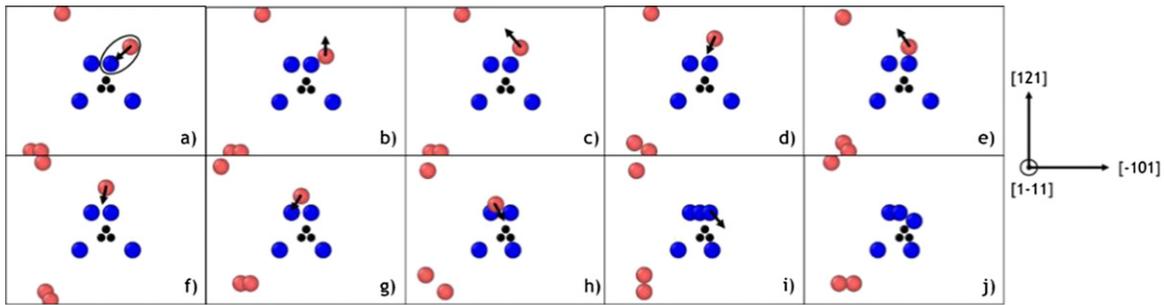
Figure 12. Mechanism showing the arrival of a C atom close to the dislocation line while being hindered by the presence of a C atom. On configuration a, the circled atoms are the atoms interacting together. The red circled atom is attracted by the dislocation line but its motion is hindered by the presence of the blue circled atom. All the other configurations show the path found by the red circled atom to finally reach the vicinity of the dislocation. The C–C distances for all the configurations are respectively 7.4 Å (a), 4.7 Å (b), 4.7 Å (c), 6.2 Å (d), 4.7 Å (e), 7.3 Å (f), 5.6 Å (g), 6.3 Å (h), 3.9 Å (i) and 6.2 Å (j). The blue atoms are the C atoms in the k-ART zone, the red atoms are the C atoms in the rigid-lattice zone, the dark atoms represent the screw dislocation and the arrows represent the C displacement. The CPU time required for the whole mechanism presented is 1.8 days for a simulated time of 153 s.
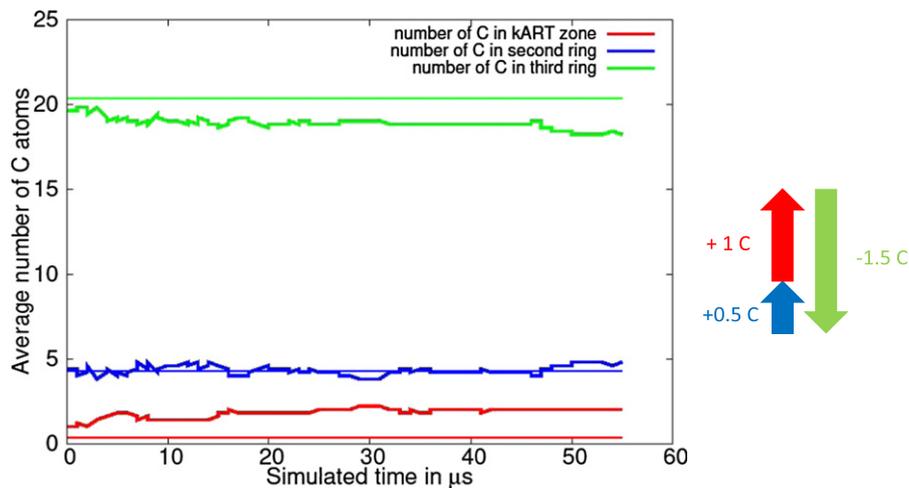

Figure 13. Average number of C atom per zone versus time for the MLKMC simulations containing 25 C atoms at 600 K with a screw dislocation in a 36 000 Fe matrix. The three zones defined are: the k-ART zone (red), the second ring (blue) and the third ring (green). The straight lines represent the concentration of C atom per zone if the C atoms formed a solid solution. The arrows represent the average C displacement between the beginning and the end of the simulations: the k-ART zone and the 2nd ring have been enriched with respectively 1 and 0.5 C atoms on average, while the 3rd ring has been depleted of 1.5 C atoms on average.

In several simulations, 2 C atoms are found to move closely to each other, despite the C–C repulsion. This appears clearly in figure 11 which shows the minimum C–C distance for all the simulations: the smallest C–C distance is observed to be below 5 Å (where 2 C atoms should start repelling each other, according to the EAM potential used, see figure 2) for several simulations. This set of configurations indicates that the sink strength of the dislocation, that tends to attract C atoms, dominates C diffusion over the C–C repulsion, which is a necessary condition for a Cottrell atmosphere to form.

The MLKMC simulation also provides interesting information about the mechanisms governing the formation of Cottrell atmospheres. For instance, C atoms in stable configurations close to the dislocation line can repel other C atoms that arrive at the dislocation vicinity. This mechanism is presented in figure 12 where a C atom close to the dislocation line [circled in configuration (a), blue circle] repels another C atom [circled in configuration (a), atom in red]. The repelled C atom finds a way to the dislocation vicinity (bumping a few times

into the C atom in a stable position), and then forces the other C atom to leave its stable position to join the final configuration (configuration *j*). This demonstrates that even if C–C repulsion is not as strong as the dislocation-induced attraction in this region (e.g. figure 12(i), the two C atoms presented are at 3.9 Å thus repelling each other), it plays a major role in the C reorganization for C atoms close to the dislocation line.

Five simulations are also launched at 600 K to study the effect of the temperature on the C migration. The evolution of the average number of C atom per zone is displayed in figure 13.

The major effect of a temperature raise on C diffusion is the significant drop in the simulation times: at 600 K, it only requires 50 μs for a second C atom to reach the dislocation vicinity (from 1 to 2 on average). However, because the sink strength of a dislocation diminishes with increasing temperature (Rauh and Simon 1978), (Rouchette *et al* 2014), the formation of a Cottrell atmosphere is not as uniform as at 300 K. Nonetheless, a comparison of the initial and final configura-
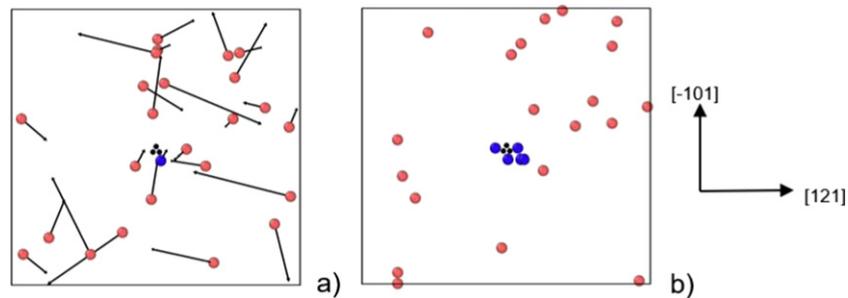
Figure 14. Initial (a) and final (b) configurations of an MLKMC simulation containing a screw dislocation and 25 C atoms at 600 K. The blue circles represent the C atoms in the k-ART zone, the red circles, those in the rigid-lattice zone and the dark circles, the screw dislocation. Computational details: each simulation requires a CPU time of 7.7 days per core (16 cores) for a simulated time of 5×10^{-5} s, 7000 steps simulation.

tions (figure 14) for one simulation, shows a clear aggregation of C atoms near the dislocation and the beginning of a Cottrell atmosphere. While the increased C mobility limits the simulated time that can be reached using MLKMC, simulation results confirm that a Cottrell atmosphere should be formed faster at 600 K than at 300 K, even with a thermally-reduced dislocation sink strength. The reduction of the dislocation sink strength is observable by comparing the C displacement per zone in figures 9 and 13: at 300 K, the C enrichment in the k-ART zone is mainly linked to C atoms going from the second ring to the k-ART zone; at 600 K, the clear drop of C concentration in the third ring indicates that C atoms arrive close to the dislocation with a lower driven force than at 300 K.

4. Conclusions

The MLKMC, which integrates a lattice-based KMC with k-ART, couples the advantages of both methods to facilitate the study of larger systems with many defects where disorder and large elastic deformation are well localised. The strength of this approach was demonstrated with the study of the onset of a C Cottrell atmosphere around a screw dislocation in bcc Fe. These simulations showed that the attraction of the dislocation is significant: from a homogeneous distribution, C atoms start aggregating around the dislocation in less than 1600 s at 300 K and less than 0.1 ms at 600 K. Moreover, while C atoms in stable positions close to the screw dislocation can provide repulsive points for other C atoms attracted by the dislocation, the C–C repulsion can be overcome by the strong deformation fields induced by disorder near the dislocation.

The MLKMC allows to speed up significantly the computational time compared to k-ART simulations for the whole system. Despite the fact that the computational cost of k-ART remains a bottleneck, this MLKMC method would be quite efficient to study kinetic phenomena driven by complex mechanisms, such as the diffusion of several interacting interstitials or solute atoms in environments distorted by extended defects (dislocations or grain boundaries), or complex activated mechanisms responsible for the motion of point defect clusters, in particular interstitial clusters with complex structures observed in Fe (Becquart *et al* 2018) and expected in other metals (Vérité

et al 2013). Efforts are currently undertaken to address these open problems.

Code availability

The MLKMC package, including the AKMC and k-ART parts, is available freely upon request to the authors.

ORCID iDs

R Candela ⬤ https://orcid.org/0000-0001-8263-9462
M Perez ⬤ https://orcid.org/0000-0002-7350-4803

References

Barkema G T and Mousseau N 1996 Event-based relaxation of continuous disordered systems *Phys. Rev. Lett.* **77** 4358

Becquart C S, Raulot J M, Bencteux G, Domain C, Perez M, Garruchet S and Nguyen H 2007 Atomistic modeling of an Fe system with a small concentration of C. *Comput. Mater. Sci.* **40** 119–29

Becquart C S, Ngayam Happy R, Olsson P and Domain C 2018 A DFT study of the stability of SIAs and small SIA clusters in the vicinity of solute atoms in Fe *J. Nucl. Mater.* **500** 92–109

Béland L K, Brommer P, El-Mellouhi F, Joly J-F and Mousseau N 2011 Kinetic activation-relaxation technique *Phys. Rev.* E **84** 046704

Béland L K *et al* 2013 Replenish and relax: explaining logarithmic annealing in ion-implanted c-Si. *Phys. Rev. Lett.* **111** 105502

Blavette D 1999 Three-dimensional atomic-scale imaging of impurity segregation to line defects *Science* **286** 2317–9

Brommer P, Béland L K, Joly J-F and Mousseau N 2014 Understanding long-time vacancy aggregation in iron: a kinetic activation-relaxation technique study *Phys. Rev.* B **90** 134109

Candela R, Becquart C S, Mousseau N, Veiga R G and Domain C 2018 Interaction between interstitial carbon atoms and an $1/2$ $\langle 1\,1\,1 \rangle$ SIA loop in an iron matrix: a combined DFT, off lattice KMC and MD study. *J. Phys.* **17** 335901

Clouet E 2007 Babel http://emmanuel.clouet.free.fr/Programs/Babel/index.html(CEA)

Cottrell A H and Bilby B A 1949 Dislocation theory of yielding and strain ageing of iron *Proc. Phys. Soc.* A **62** 49

Domain C, Becquart C S and Foct J 2004 *Ab initio* study of foreign interstitial atom (C, N) interactions with intrinsic point defects in α-Fe *Phys. Rev.* B **69** 144112

De A K, De Blauwe K, Vandeputte S and De Cooman B C 2000 Effect of dislocation density on the low temperature aging behavior of an ultra low carbon bake hardening steel *J. Alloys Compd.* **310** 405–10

El-Mellouhi F, Mousseau N and Lewis L J 2008 Kinetic activation-relaxation technique: an off-lattice self-learning kinetic Monte Carlo algorithm *Phys. Rev.* B **78** 153202

Kang H C and Weinberg W H 1989 Dynamic Monte Carlo with a proper energy barrier: surface diffusion and two-dimensional domain ordering *J. Chem. Phys.* **90** 2824–30

Li W-Y, Zhang Y, Zhou H-B, Jin S and Lu G-H 2011 Stress effects on stability and diffusion of H in W: a first-principles study *Nucl. Instrum. Methods Phys. Res.* B **269** 1731

Liu Y-L, Zhou H-B and Zhang Y 2011 Investigating behaviors of H in a W single crystal by first-principles: from solubility to interaction with vacancy *J. Alloys Compd.* **509** 8277

Malek R and Mousseau N 2000 Dynamics of Lennard-Jones clusters: a characterization of the activation-relaxation technique *Phys. Rev.* E **62** 7723

Massardier V, Lavaire N, Soler M and Merlin J 2004 Comparison of the evaluation of the carbon content in solid solution in extra-mild steels by thermoelectric power and by internal friction *Scr. Mater.* **50** 1435–9

McKay B D 1981 Practical graph isomorphism *Congr. Numerantium* **30** 45–87

Miller M K 2006 Atom probe tomography characterization of solute segregation to dislocations *Microsc. Res. Tech.* **69** 359–65

Mousseau N and Barkema G T 1998 Traveling through potential energy landscapes of disordered materials: the activation-relaxation technique *Phys. Rev.* E **57** 2419–24

Mousseau N, Béland L K, Brommer P, El-Mellouhi F, Joly J-F, N'Tsouaglo G K, Restrepo O and Trochet M 2015 Following atomistic kinetics on experimental timescales with the kinetic activation-relaxation technique *Comput. Mater. Sci.* **100** 111–23

Rauh H and Simon D 1978 On the diffusion process of point defects in the stress field of edge dislocations *Phys. Status Solidi* A **46** 499–510

Restrepo O A, Mousseau N, El-Mellouhi F, Bouhali O, Trochet M and Becquart C S 2016 Diffusion properties of Fe–C systems studied by using kinetic activation-relaxation technique *Comput. Mater. Sci.* **112** 96–106

Restrepo O A, Mousseau N, Trochet M, El-Mellouhi F, Bouhali O and Becquart C S 2018 Carbon diffusion paths and segregation at high-angle tilt grain boundaries in α-Fe studied by using a kinetic activation-relation technique *Phys. Rev.* B **97** 054309

Rouchette H, Thuinet L, Legris A, Ambard A and Domain C 2014 Quantitative phase field model for dislocation sink strength calculations *Comput. Mater. Sci.* **88** 50–60

Smith G D W, Hudson D, Styman P D and Williams C A 2013 Studies of dislocations by field ion microscopy and atom probe tomography *Phil. Mag.* **93** 3726–40

Tchitchekova D S, Morthomas J, Ribeiro F, Ducher R and Perez M 2014 A novel method for calculating the energy barriers for carbon diffusion in ferrite under heterogeneous stress *J. Chem. Phys.* **141** 034118

Van der Ven A, Ceder G, Asta M and Tepesch P D 2001 First-principles theory of ionic diffusion with nondilute carriers *Phys. Rev.* B **64** 184307

Veiga R G A, Perez M, Becquart C S, Domain C and Garruchet S 2010 Effect of the stress field of an edge dislocation on carbon diffusion in α-iron: coupling molecular statics and atomistic kinetic Monte Carlo *Phys. Rev.* B **82** 054103

Veiga R G A, Perez M, Becquart C S, Clouet E and Domain C 2011 Comparison of atomistic and elasticity approaches for carbon diffusion near line defects in α-iron *Acta Mater.* **59** 6963–74

Veiga R G A, Becquart C S and Perez M 2014 Comments on 'Atomistic modeling of an Fe system with a small concentration of C' *Comput. Mater. Sci.* **82** 118–21

Veiga R G A, Goldenstein H, Perez M and Becquart C S 2015 Monte Carlo and molecular dynamics simulations of screw dislocation locking by Cottrell atmospheres in low carbon Fe–C alloys *Scr. Mater.* **108** 19–22

Vérité G, Domain C, Chu-Chun F, Gasca P, Legris A and Willaime F 2013 Self-interstitial defects in hexagonal close packed metals revisited: evidence for low-symmetry configurations in Ti, Zr, and Hf *Phys. Rev.* B **87** 134108

Vincent E, Becquart C S, Pareige C, Pareige P and Domain C 2008 Precipitation of the FeCu system: a critical review of atomic kinetic Monte Carlo simulations *J. Nucl. Mater.* **373** 387–401

Waseda O, Veiga R G, Morthomas J, Chantrenne P, Becquart C S, Ribeiro F, Jelea A, Goldenstein H and Perez M 2017 Formation of carbon Cottrell atmospheres and their effect on the stress field around an edge dislocation *Scr. Mater.* **129** 16–9

Wilde J, Cerezo A and Smith G D W 2000 Three-dimensional atomic-scale mapping of a Cottrell atmosphere around a dislocation in iron *Scr. Mater.* **43** 39–48